Original Article

Myocardial work and energy loss of left ventricle obtained by pressure-strain loop and vector flow mapping: a new perspective on idiopathic left bundle branch block

Yu Gao[1,2#^], Yanjuan Zhang[1#], Yihu Tang[3#], Hongping Wu[1], Fang Xu[1], Jian Hong[4], Di Xu[4]

[1]Department of Cardiology, The First Affiliated Hospital of Nanjing Medical University, Nanjing, China; [2]Department of Cardiology, The Second People's Hospital of Hefei, Hefei Hospital Affiliated to Anhui Medical University, Hefei, China; [3]Department of Cardiovascular Surgery, The First Affiliated Hospital of Nanjing Medical University, Nanjing, China; [4]Department of Geriatrics, The First Affiliated Hospital of Nanjing Medical University, Nanjing, China

Contributions: (I) Conception and design: Y Gao, D Xu, J Hong; (II) Administrative support: Y Zhang, Y Tang, D Xu; (III) Provision of study materials or patients: Y Tang, H Wu, F Xu; (IV) Collection and assembly of data: Y Zhang, Y Gao; (V) Data analysis and interpretation: Y Zhang; (VI) Manuscript writing: All authors; (VII) Final approval of manuscript: All authors.

[#]These authors contributed equally to this work.

Correspondence to: Di Xu; Jian Hong. Department of Geriatrics, The First Affiliated Hospital of Nanjing Medical University, 300 Guangzhou Road, Nanjing 210029, China. Email: xudi@jsph.org.cn; hongjian@jsph.org.cn.

Background: To date, no research has been conducted on the electrical activity and mechanical dyssynchrony of idiopathic left bundle branch block (iLBBB) with normal left ventricular ejection fraction (LVEF). This study sought to assess the left ventricular summation of energy loss (EL-SUM) and average energy loss (EL-AVE) using vector flow mapping as well as myocardial work using pressure-strain loop (PSL) in patients with iLBBB and normal LVEF.

Methods: We prospectively recruited 35 patients with iLBBB and 35 control participants with normal LVEF. Echocardiography was performed. Conventional echocardiographic parameters, myocardial work, and energy loss (i.e., the EL-SUM and EL-AVE) were calculated.

Results: In relation to global myocardial work, compared to the control participants, the iLBBB patients showed decreased global longitudinal strain (GLS; –15.32%±2.58% *vs.* –18.27%±2.12%; P=0.001), a decreased global work index (GWI; 1,428.24±338.18 *vs.* 1,964.87±264.16 mmHg%; P<0.001), decreased global work efficiency (GWE) (84.48±5.19 *vs.* 91.73±5.31 mmHg%; P<0.001), and significantly increased global waste work (GWW; 341.60±132.62 *vs.* 161.80±106.81 mmHg%; P<0.001). In relation to the regional index, the iLBBB patients had a significantly reduced basal anteroseptal segment (879.15±370.50 *vs.* 1,746.38±154.44 mmHg%; P<0.001), basal inferoseptal segment (1,111.42±389.04 *vs.* 1,677.25±223.10 mmHg%; P<0.001), mid-anteroseptal segment (1,097.54±394.83 *vs.* 1,815.06±291.22 mmHg%; P<0.001), mid-inferoseptal segment (1,012.54±353.33 *vs.* 1,880.88±254.39 mmHg%; P<0.001), apical anterior segment (1,592.42±366.64 *vs.* 1,910.00±170.27 mmHg%; P=0.001), apical lateral segment (1,481.62±342.95 *vs.* 1,817.19±227.55 mmHg%; P=0.001), apical septal segment (1,437.65±428.22 *vs.* 1,852.25±275.19 mmHg%; P=0.001), and apex (1,542.62±342.89 *vs.* 1,907.06±197.94 mmHg%; P<0.001). The iLBBB patients had increased EL-AVE and EL-SUM during the late-diastole, isovolumic-systole, and rapid-ejection periods [EL-AVE in T2: 28.3 (8.7, 49.0) *vs.* 6.8 (5.4, 9.4) J/(s·m^3); P=0.029]; [EL-AVE in T3: 24.7 (13.0, 46.8) *vs.* 7.2 (5.4,

^ ORCID: 0000-0001-8011-5446.

10.8) J/(s·m^3), P<0.001]; [EL-AVE in T4: 18.3 (12.0, 27.6) *vs.* 7.7 (4.1, 11.6) J/(s·m^3), P=0.002]; [EL-SUM in T2: 8.3 (2.2, 14.5) *vs.* 2.1 (1.6, 3.2) J/(s·m), P=0.049]; [EL-SUM in T3: 7.6 (4.0, 14.5) *vs.* 2.2 (1.7, 3.3) J/(s·m), P<0.001]; [EL-SUM in T4: 5.3 (3.6, 9.7) *vs.* 2.2 (1.4, 3.0) J/(s·m), P=0.004].

Conclusions: The GWI and GWE were reduced in patients with iLBBB, especially in the septum and apex. The EL-SUM and EL-AVE were higher in patients with iLBBB during the late-diastole, isovolumic-systole, and rapid-ejection periods. EL and PSL reflect the LV hemodynamics of patients with iLBBB.

Keywords: Left bundle branch block (LBBB); energy loss; left ventricular; echocardiography; vector flow mapping

Submitted Mar 27, 2022. Accepted for publication Oct 14, 2022. Published online Nov 07, 2022.
doi: 10.21037/qims-22-284
View this article at: https://dx.doi.org/10.21037/qims-22-284

Introduction

Left bundle branch block (LBBB) is a characteristic model of ventricular electromechanical dyssynchrony. It is associated with increased risk of cardiovascular disease, ventricular dysfunction, heart failure and higher mortality than people without LBBB (1-3). In the overall population, the prevalence of LBBB is <1% (4), but by the age of 80 years, it increases to 17% (5). LBBB is usually associated with structural heart disease, coronary artery disease, or cardiomyopathy. Idiopathic left bundle branch block (iLBBB) may be present in individuals without detectable cardiovascular disease and has a prevalence rate of 0.1% in the general population (6,7). In patients with LBBB, structural heart disease, and iLBBB, the dyssynchronous electrical activation of the left ventricle (LV) may stimulate progressive LV structural remodeling and lead to heart failure (8). A case-control study by Sze *et al.* (9) showed a significant decrease in the left ventricular ejection fraction (LVEF) of patients with LBBB compared to controls. Over a 3.8-year follow-up period, 36% of the patients in the LBBB groups showed a reduction in LVEF of <45%, while only 10% of the controls showed a reduction in LVEF. Some studies have shown that due to LV electromechanical dyssynchrony, patients with iLBBB present with reduced LVEF and increased LV volumes compared to healthy controls. iLBBB caused structural remodeling, left ventricular dysfunction, and eventually heart failure (1). Conversely, others (10,11) have found that iLBBB is associated with a low mortality rate and incidence of cardiomyopathy. Given these paradoxical results, it is essential to more clearly understand the electromechanical activity of the left ventricle in patients with iLBBB. The electrical activity and mechanical dyssynchrony of iLBBB, which slowly affects LV function, cannot be ignored, especially in those with normal LVEF. This study sought to observe the changes in the hemodynamics of patients with iLBBB and normal LVEF from the perspective of left ventricular myocardial work and left ventricular energy loss (EL). To achieve our objective, we used novel techniques to assess the LV electromechanical activity and cardiac function of patients with iLBBB.

Noninvasive LV myocardial work based on the pressure-strain loop (PSL) can be used to quantify regional myocardial work (12). Using brachial blood pressure instead of left ventricular pressure, this method was applied to 2-dimensional (2D) speckle tracking technology to generate a left ventricular strain curve, and the left ventricular strain and pressure were then integrated to estimate the myocardial work. Mechanical dyssynchrony affects intracardiac hemodynamics, which can be visualized and evaluated by magnetic resonance imaging (12), particle imaging velocimetry (13), and vector flow mapping (VFM). In 2013, Itatani *et al.* (14) modified the 2D speckle tracking technique by applying it to VFM and used the continuum equation to calculate the blood flow vector to obtain the energy dissipation from the viscous friction of blood flow. The intraventricular energy dissipation represents an additional EL due to the friction of blood flow within the LV, which is a type of LV workload. The EL represents the consumption of blood flow energy caused by fractions of blood in the turbulent flow and can be used to predict both the ventricular load in various heart diseases and the spatial dispersion of blood flow signal in the ventricle. VFM is a novel approach for visualizing and quantitatively evaluating intraventricular flow velocity vectors using color Doppler and speckle tracking data (14). Previous studies have reported on the EL of the LV in a variety of different

diseases. For instance, one study reported that patients with aortic regurgitation showed higher EL than did normal patients during diastole (15). Calculating the loss of energy derived from the intraventricular flow velocity vector field, which reflects viscous dissipation in turbulent blood (14), can provide a new perspective on changes in heart function.

This study evaluated the LV motion pattern of patients with iLBBB from the perspective of myocardial work and EL based on the 2 techniques mentioned above to gain a deeper understanding of the electromechanical activity for use in clinical settings.

Methods

Patients

Between January 2018 and December 2019, 70 patients at the Cardiology Department of The First Affiliated Hospital of Nanjing Medical University were prospectively recruited and divided into the following two groups: (I) the iLBBB group and (II) the control group. To be eligible for inclusion in the iLBBB group, the patients had to meet the following inclusion criteria: (I) be aged over 18 years; (II) meet the LBBB criteria (see below); and (III) have LVEF >50%. The LBBB criteria were as follows: a complete LBBB, which was defined as a QRS duration of ≥140 ms in men and ≥130 ms in women; a negative terminal deflection in leads V1 and V2 (QS or rS) and mid-QRS complex slowing or notching in leads V1, V2, V5, V6, I, and aVL (16). Patients were excluded from the study if they met any of the following criteria: (I) had a history of or evidence indicating a diagnosis of coronary heart disease, valvular heart disease, or hypertrophic cardiomyopathy; (II) had a cardiac pacemaker implantation; (III) had poor quality ultrasound images; and/or (IV) had a non-sinus rhythm. Patients enrolled in the control group were matched to those in the iLBBB group in terms of gender, age, height, LVEF, and weight. The study was conducted in accordance with the Declaration of Helsinki (as revised in 2013). The study was approved by the Institutional Review Board of The First Affiliated Hospital of Nanjing Medical University, and informed consent was obtained from all the individual participants.

Electrocardiography

All the participants underwent a standard, resting 12-lead electrocardiogram (ECG; Hewlett-Packard Pagewriter XIi). The QRS duration was measured from the beginning to the end of the QRS complex with simultaneous 12-lead ECG signals (maximum QRS; high-pass filter 0.05 Hz; low-pass filters 150 Hz, 100 mm/mV, and 25 mm/s). All digital data were transferred to two different cardiologists for interpretation.

Blood pressure

All the participants were seated, and after they had rested for >20 minutes, an electronic sphygmomanometer cuff (Omron HEM-7124) was placed over the right upper extremity. The height of the cuff was at the same level as the heart. The blood pressure was manually obtained by pressing the start button. The measurements of all the participants were taken 3 times, and the average value was recorded.

Echocardiography

We used the GE Vivid E95 and Hitachi Aloka Prosound F75 color Doppler ultrasound machines equipped with an M5S probe and a UST-52105 probe, respectively. Conventional echocardiographic parameters and LV myocardial work parameters as quantified by the LV PSL were measured by the GE Vivid E95 with an M5S probe. EL was measured by VFM using the Hitachi Aloka Prosound F75 with the UST-52105 probe.

All the participants underwent echocardiography in the left lateral decubitus position connecting with the ECG electrodes. All the images were ECG-triggered and stored with 3 consecutive cardiac cycles. The GE VIVID E95 was used to measure conventional echocardiographic parameters by experienced sonographers. All the 2D echocardiographic parameters represented the average of 3 consecutive cardiac cycles and were performed according to current recommendations. LVEF was measured using Simpson's biplane method (17). The collected echocardiographic measurements included peak blood flow velocities at the mitral valve during early filling (E wave) and late diastole (A wave). The E/e' ratio was the average value of the E wave separately divided by the peak myocardial velocities at the septal mitral annulus and lateral mitral annulus.

LV myocardial work by quantification of the LV PSL

Dynamic images of 3 consecutive cardiac cycles in apical 4-chamber, 2-chamber, and 3-chamber views, as well as

dynamic images of the mitral and aortic valve flow spectrum were imported into Echopac software (GE Healthcare). The strain values were measured by automatic functional imaging. The system automatically selected the apical views, and the endocardial and epicardial boundaries were automatically tracked by the software in sequence. If the automatic tracing failed, the endocardial and epicardial boundaries were manually traced. Next, 17-segment strain curves and bull's-eye diagrams of the LV were automatically generated. To analyze the myocardial work, the blood pressure values were entered into the software, and the standardized reference curve was adjusted according to the different cardiac cycle phases (i.e., the isovolumic-systole and ejection phase based on aortic and mitral valve opening and closing times), resulting in the myocardial PSL curve and the myocardial work parameter values. The overall parameters were global longitudinal strain (GLS), the global work index (GWI), global constructive work (GCW), global waste work (GWW), and global work efficiency (GWE). The segmental parameter was the myocardial work index (MWI), which was calculated for each segment based on the bull's-eye diagram (*Figure 1*).

EL by vector flow mapping

Images for flow visualization were acquired in the VFM mode in an apical 3-chamber view, 4-chamber view, and 2-chamber view of 3 consecutive cardiac cycles using the Hitachi Aloka Prosound F75. The probe frequency and depth were dynamically adjusted, while the image frame rate was kept at 25 frames per second. We ensured that the blood flow sampling frame surrounded the entire LV. Blood flow images at the apical long-axis, 4-chamber, and 2-chamber views were obtained within 3 consecutive cardiac cycles at a frame frequency >18 Hz by VFM. The images covered the entire LV. The VFM images were stored in DICOM file format for off-line analysis using the commercially available VFM analysis software DAS-RS1 (Hitachi Aloka Medical Ltd.). The ventricular endocardial boundary was manually traced with the software by applying 2D speckle tracking throughout the entire cardiac cycle. If the aliasing phenomenon was observed in the color Doppler data, the aliased area was manually corrected. After the region of interest was determined by tracing the entire LV, the EL distribution was displayed. The blood flow EL was defined as the energy of frictional heat generated due to viscosity at the sites at which turbulent flow occurred. EL was the most significant at the sites at which a considerable change of vectors was locally observed and the smallest at the laminar flow site. From the velocity vector fields of the intraventricular blood flow, the EL was calculated for each frame of the cine loop image. EL was calculated as follows:

$$EL = \sum_{i,j} \int u \left(\frac{\partial u_i}{\partial x_i} + \frac{\partial u_j}{\partial x_i} \right)^2 dv \quad [1]$$

where μ represents the blood viscosity coefficient, which was set as 0.004 Pa·s, and i and j represent the coordinates of the 2D Cartesian coordinate system (18). The total EL (EL-SUM) and the average EL (EL-AVE) were calculated for each time phase and each segment by tracing the basal, mid, and apical segments of the LV using the formula established by Itatani *et al.* (14), as shown in *Figure 2*. The EL-AVE indicates the EL per square meter (*Figure 2*).

Heart rate was calculated based on the R-wave interval of the cardiac cycle on the ECG. During the cardiac cycle, the following 4 points were determined by combining the ECG, valve opening time, and time-flow curve: early diastole period (rapid filling) (T1), late-diastole period (atrial systole) (T2), isovolumic-systole period (T3), and rapid-ejection period (T4). During the T1, T2, T3, and T4, the following indices were measured: EL-AVE and EL-SUM.

Reproducibility

The intra- and interobserver variability for EL in different locations and myocardial work in different segments was analyzed repeatedly in 10 randomly selected participants. The repeat analysis was performed more than 7 days after the initial analysis. To assess intraobserver variability, 1 observer evaluated the same studies on 2 separate occasions. To assess interobserver variability, 2 independent observers performed the analyses separately.

Statistical analyses

All the data were analyzed using SPSS 24.0 (IBM Corp.). The continuous variables are presented as the mean ± standard deviation or median (interquartile range), and the categorical data are presented as the percentage or frequency. The continuous data with a normal distribution were compared using the Student t test, and those with a non-normal distribution were compared using the Mann-Whitney test. The categorical variables across the groups were compared using the chi-square test. A P value <0.05 was considered statistically significant for all tests.

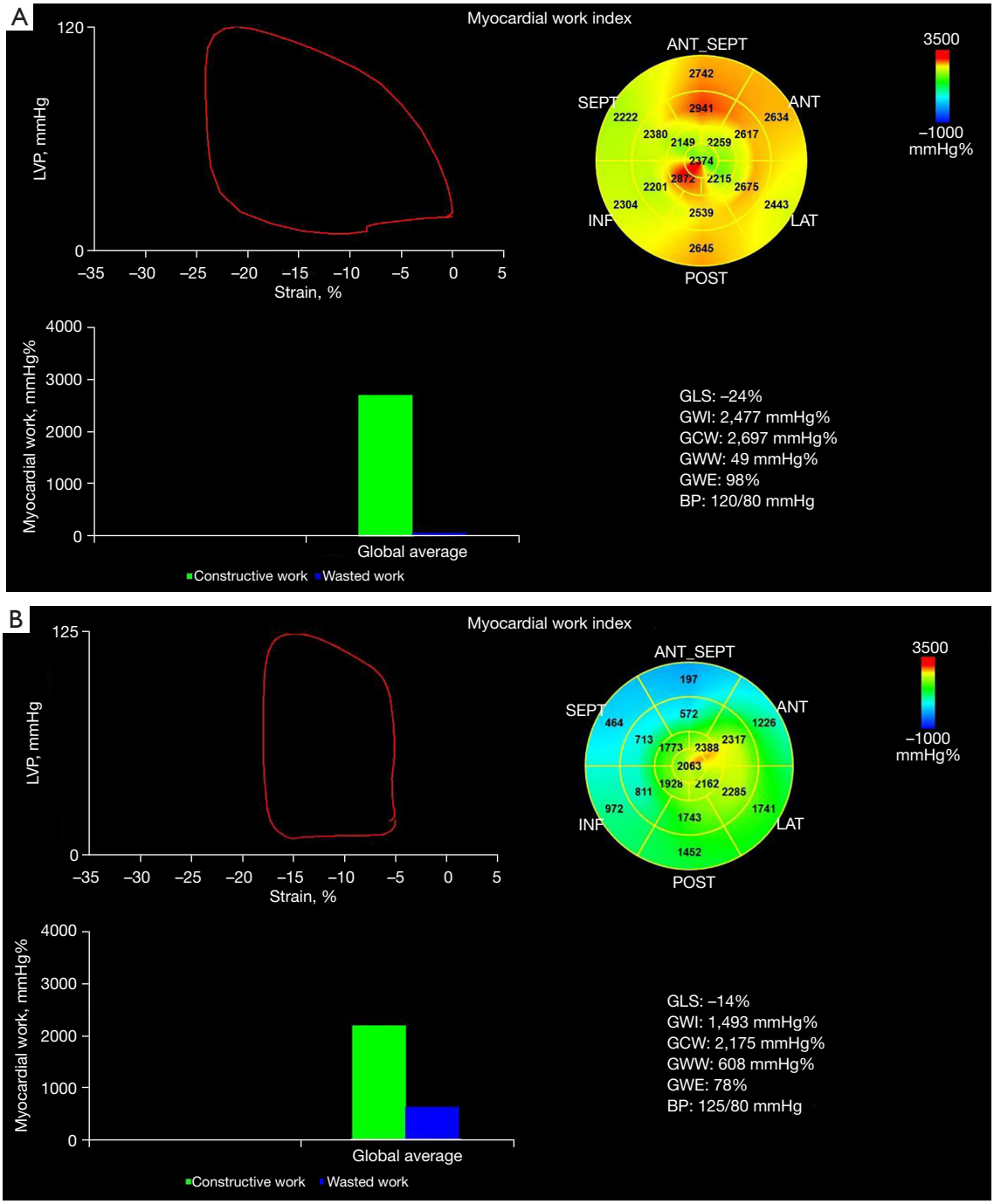

Figure 1 Parameters of myocardial work. (A) Control; (B) iLBBB. LVP, left ventricle pressure; ANT_SEPT, anteroseptal; INF, inferior; LAT, lateral; POST, posterior; GLS, global longitudinal strain; GCW, global constructive work; GWW, global waste work; GWE, global work efficiency; BP, blood pressure; iLBBB, idiopathic left bundle branch block.

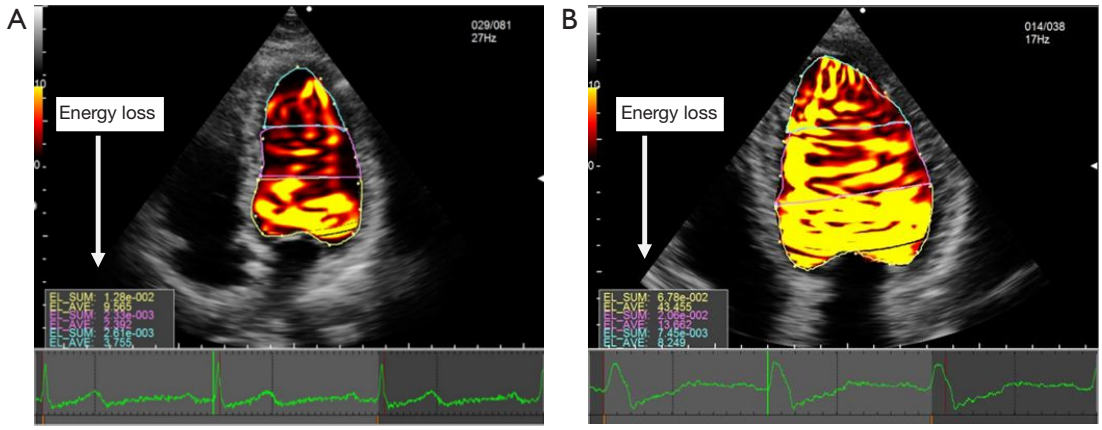

Figure 2 The EL-SUM and the EL-AVE at the basal, mid, and apical segments during the isovolumic-systole period. (A) Control; (B) iLBBB. EL-SUM, summation of energy loss; EL-AVE, average energy loss; iLBBB, idiopathic left bundle branch block.

Results

General characteristics

The demographic and echocardiographic characteristics of the participants are listed in *Table 1*. We enrolled 35 patients with iLBBB (20 males and 15 females) and matched them to 35 controls in this study. The QRS duration was significantly longer in the iLBBB patients than in the controls (154.68±12.56 *vs.* 91.07±3.83 s; P<0.001). E/A (the ratio of peak velocity blood flow from left ventricular relaxation in early diastole (the E wave) to peak velocity flow in late diastole caused by atrial contraction (the A wave) was significantly lower in the patients with iLBBB than in the controls (0.71±0.05 *vs.* 0.92±0.18; P=0.008). No significant differences were observed in the other parameters between the controls and the patients with idiopathic LBBB (*Table 1*).

Left ventricular myocardial work

In relation to global myocardial work, compared to the controls, the patients with iLBBB showed decreased GLS (–15.32%±2.58% *vs.* –18.27%±2.12%; P=0.001), a decreased GWI (1,428.24±338.18 *vs.* 1,964.87±264.16 mmHg%; P<0.001), decreased GWE (84.48±5.19 *vs.* 91.73±5.31 mmHg%; P<0.001), and significantly increased GWW (341.60±132.62 *vs.* 161.80±106.81 mmHg%; P<0.001; *Table 2*). In relation to the regional index, the patients with iLBBB had significantly reduced segmental MWIs of the basal anteroseptal segment (879.15±370.50 *vs.* 1,746.38±154.44 mmHg%; P<0.001), basal inferior segment (1,391.54±421.52 *vs.* 1,749.94±257.82 mmHg%, P=0.004), basal inferoseptal segment (1,111.42±389.04 *vs.* 1,677.25±223.10 mmHg%; P<0.001), mid-anteroseptal segment (1,097.54±394.83 *vs.* 1,815.06±291.22 mmHg%; P<0.001), mid-inferior segment (1,207.54±290.83 *vs.* 1,882.44±195.53 mmHg%; P<0.001), mid-inferoseptal segment (1,012.54±353.33 *vs.* 1,880.88±254.39 mmHg%; P<0.001), apical anterior segment (1,592.42±366.64 *vs.* 1,910.00±170.27 mmHg%; P=0.001), apical lateral segment (1,481.62±342.95 *vs.* 1,817.19±227.55 mmHg%; P=0.001), apical septal segment (1,437.65±428.22 *vs.* 1,852.25±275.19 mmHg%; P=0.001), and apex (1,542.62±342.89 *vs.* 1,907.06±197.94 mmHg%; P<0.001; *Table 3*).

The patients with iLBBB showed increased EL-AVE and EL-SUM levels in the T2, T3, and T4: [EL-AVE in T2: 28.3 (8.7, 49.0) *vs.* 6.8 (5.4, 9.4) J/(s·m^3); P=0.029]; [EL-AVE in T3: 24.7 (13.0, 46.8) *vs.* 7.2 (5.4, 10.8) J/(s·m^3), P<0.001]; [EL-AVE in T4: 18.3 (12.0, 27.6) *vs.* 7.7 (4.1, 11.6) J/(s·m^3), P=0.002]; [EL-SUM in T2: 8.3 (2.2, 14.5) *vs.* 2.1 (1.6, 3.2) J/(s·m), P=0.049]; [EL-SUM in T3: 7.6 (4.0, 14.5) *vs.* 2.2 (1.7, 3.3) J/(s·m), P<0.001]; [EL-SUM in T4: 5.3 (3.6, 9.7) *vs.* 2.2 (1.4, 3.0) J/(s·m), P=0.004]. No significant differences were found between the two groups in the T1. The most notable difference was observed in the T3 (P<0.001) (*Tables 4,5*).

The EL-AVE and EL-SUM levels in the basal segment of the patients with iLBBB increased considerably throughout the T2, T3, and T4. Notably, the EL-AVE level increased significantly during the T3 (P<0.001). The EL-AVE and EL-SUM levels in the middle segment increased during the T2, T3, and T4; and the EL-SUM

Table 1 Participants demographic and echocardiographic characteristics

Variables	Normal (N=35), mean ± SD	iLBBB (N=35), mean ± SD	*t*	P
Age (years)	64.33±5.92	68.56±11.38	–1.330	0.192
Height (cm)	167.27±8.19	164.36±7.39	1.157	0.255
Weight (kg)	64.47±8.69	62.04±8.88	0.843	0.404
QRS (s)	91.07±3.83	154.68±12.56	–19.012	<0.001*
LVEF (%)	63.47±1.63	62.35±2.30	1.258	0.224
SBP (mmHg)	123.33±9.56	121.96±5.97	0.561	0.578
DBP (mmHg)	77.87±4.87	77.08±6.52	0.404	0.689
HR (bpm)	72.60±9.18	73.84±8.42	–0.436	0.665
LAD (mm)	32.70±3.50	34.60±5.76	–0.892	0.384
LVDd (mm)	45.70±3.50	47.10±3.60	–0.882	0.39
IVS (mm)	9.80±1.03	10.50±0.97	–1.561	0.136
LVPW (mm)	9.60±0.84	10.20±0.920	–1.521	0.146
RAD (mm)	32.00±2.36	31.40±2.50	0.552	0.588
RVDd (mm)	31.60±1.90	32.60±2.91	–0.910	0.375
E (cm/s)	77.20±12.24	69.80±9.83	1.491	0.153
A (cm/s)	80.00±29.06	96.60±17.80	–1.541	0.141
E/A	0.92±0.18	0.71±0.05	3.379	0.008*
E/e’	8.79±2.04	10.31±3.06	–1.308	0.207
TAPSE (mm)	20.50±0.97	19.60±0.97	2.077	0.051
TR (cm/s)	2.35±0.12	2.50±0.20	–2.043	0.056

*, P<0.05. iLBBB, idiopathic left bundle branch block; mean ± SD, mean ± standard deviation; QRS, Q wave, R wave and S wave; LVEF, left ventricular ejection fraction; SBP, systolic pressure; DBP, diastolic pressure; HR, heart rate; LAD, left atrial diameter; LVDd, left ventricular end diastolic dimension; IVS, interventricular septum; LVPW, left ventricular posterior wall; RAD, right atrial diameter; RVDd, right ventricular end diastolic dimension; E/A, the ratio of peak blood flow velocities at the mitral valve during early filling (E wave) and late diastole (A wave); e’, early diastolic mitral annular tissue velocity; TAPSE, tricuspid annular plane systolic excursion; TR, tricuspid regurgitation.

Table 2 Left ventricular myocardial work

Variables	Normal (N=35), mean ± SD	iLBBB (N=35), mean ± SD	*t*	P
GLS (%)	–18.27±2.12	–15.32±2.58	–3.730	0.001*
GWI (mmHg%)	1,964.87±264.16	1,428.24±338.18	5.25	<0.001*
GCW (mmHg%)	2,036.27±278.81	1,926.40±344.55	1.045	0.303
GWW (mmHg%)	161.80±106.81	341.60±132.62	–4.449	<0.001*
GWE (%)	91.73±5.31	84.48±5.19	4.243	<0.001*

*, P<0.05. iLBBB, idiopathic left bundle branch block; mean ± SD, mean ± standard deviation; GLS, global longitudinal strain; GWI, global work index; GCW, global constructive work; GWW, global waste work; GWE, global work efficiency.

Table 3 Myocardial work index of each segment

Variables	Myocardial work index, mmHg%, mean ± SD		t	P
	Normal	iLBBB		
Basal anteroseptal	1,746.38±154.44	879.15±370.50	10.54	<0.001*
Basal anterior	1,795.19±195.18	1,611.19±408.63	1.961	0.057
Basal anterolateral	1,768.38±211.63	1,748.42±375.96	0.22	0.827
Basal inferolateral	1,747.81±257.96	1,748.73±433.93	–0.008	0.994
Basal inferior	1,749.94±257.82	1,391.54±421.52	3.059	0.004*
Basal inferoseptal	1,677.25±223.10	1,111.42±389.04	5.987	<0.001*
Mid-anteroseptal	1,815.06±291.22	1,097.54±394.83	6.282	<0.001*
Mid-anterior	1,828.25±231.89	1,714.23±394.24	1.18	0.245
Mid-anterolateral	1,780.13±278.71	1,666.73±335.71	1.131	0.265
Mid-inferolateral	1,787.00±283.84	1,652.77±382.02	1.212	0.232
Mid-inferior	1,882.44±195.53	1,207.54±290.83	8.194	<0.001*
Mid-inferoseptal	1,880.88±254.39	1,012.54±353.33	8.544	<0.001*
Apical anterior	1,910.00±170.27	1,592.42±366.64	3.801	0.001*
Apical lateral	1,817.19±227.55	1,481.62±342.95	3.465	0.001*
Apical inferior	1,740.25±214.07	1,630.42±375.66	1.065	0.293
Apical septal	1,852.25±275.19	1,437.65±428.22	3.45	0.001*
Apex	1,907.06±197.94	1,542.62±342.89	3.863	<0.001*

*, P<0.05. iLBBB, idiopathic left bundle branch block; SD, standard deviation.

Table 4 EL-AVE in the control group and the LBBB group

Variables	EL-AVE, J/(s·m^3), median (IQR)		P
	Normal	iLBBB	
T1	12.8 (9.3, 23.2)	13.8 (4.7, 34.3)	0.912
T2	6.8 (5.4, 9.4)	28.3 (8.7, 49.0)	0.029*
T3	7.2 (5.4, 10.8)	24.7 (13.0, 46.8)	<0.001***
T4	7.7 (4.1, 11.6)	18.3 (12.0, 27.6)	0.002**

*P<0.05, **P<0.01, ***P<0.001 *vs.* control group. EL-AVE, average energy loss; LBBB, left bundle branch block; iLBBB, idiopathic left bundle branch block; IQR, interquartile range; T1, early diastole period; T2, late-diastole period; T3, isovolumic-systole period; T4, rapid-ejection period.

levels increased the most during the T3 and T4 (P<0.001). The apex also showed increased EL-AVE and EL-SUM levels during the T2, T3, and T4, among which the EL-SUM level was the most prominent during the T3 and T4 (P<0.001; *Figures 3*,*4*).

Reproducibility

Inter- and intraobserver variability showed good reproducibility. The interclass correlation coefficients were all >0.8, which indicated that the myocardial work and EL

Table 5 EL-SUM in the control group and the LBBB group

Variables	EL-SUM, J/(s·m), median (IQR)		P
	Normal	iLBBB	
T1	3.4 (2.8, 7.7)	3.5 (1.7, 7.7)	0.739
T2	2.1 (1.6, 3.2)	8.3 (2.2, 14.5)	0.049*
T3	2.2 (1.7, 3.3)	7.6 (4.0, 14.5)	<0.001***
T4	2.2 (1.4, 3.0)	5.3 (3.6, 9.7)	0.004**

*P<0.05, **P<0.01, ***P<0.001 *vs.* control group. EL-SUM, summation of energy loss; LBBB, left bundle branch block; iLBBB, idiopathic left bundle branch block; IQR, interquartile range; T1, early diastole period; T2, late-diastole period; T3, isovolumic-systole period; T4, rapid-ejection period.

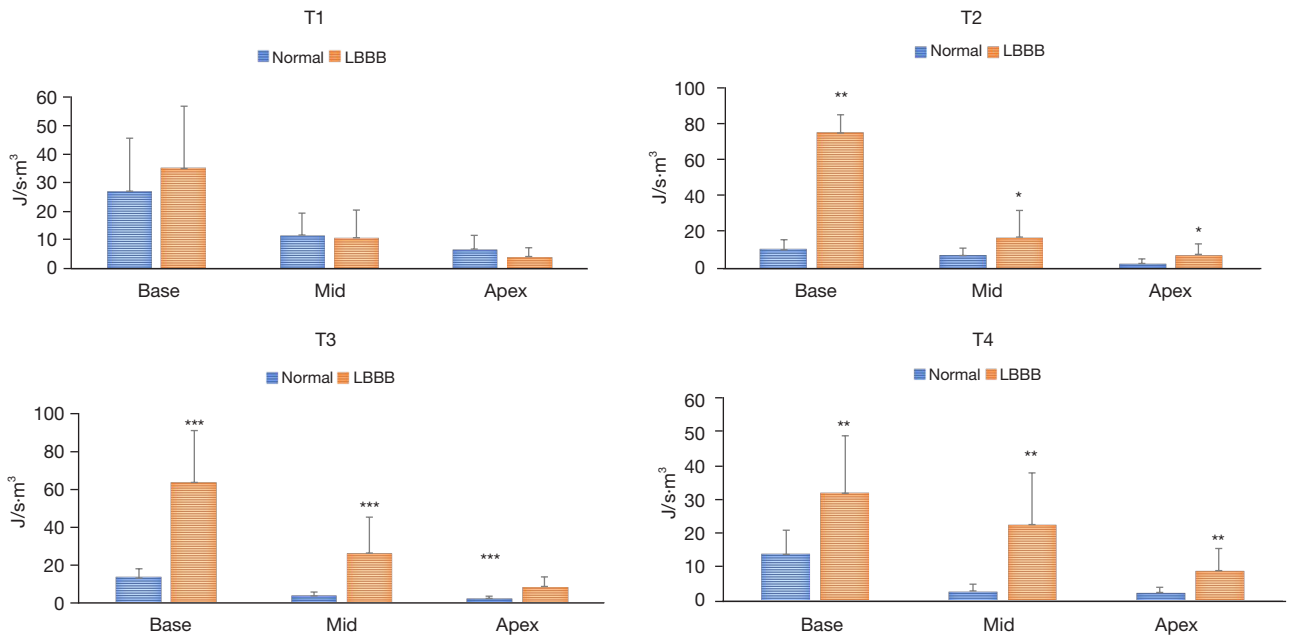

Figure 3 EL-AVE in the basal (EL-base), mid (EL-mid), and apical (EL-apex) segments of the left ventricle in the control group and the iLBBB group (J/s·m^3). *P<0.05; **P<0.01; ***P<0.001. T1, early diastole period; T2, late-diastole period; T3, isovolumic-systole period; T4, rapid-ejection period; LBBB, left bundle branch block; EL-AVE, average energy loss.

measurements had high reliability and repeatability (*Table 6*).

Discussion

As recently demonstrated, normal LVEF in patients with LBBB does not always represent normal systolic function (18). The dyssynchronous electrical activity of LBBB affects the mechanical systolic function of LV. We analyzed the LV myocardial work using the PSL technique to observe the LV functional changes in patients with iLBBB and normal LVEF. Strain refers to the change in morphology of a solid substance under an external force. This parameter is load-dependent. It has been shown that an increase in afterload leads to a decrease in strain (19). A previous study (20) showed that strain varies after dialysis because of the preload changes.

The PSL is a new noninvasive parameter that can be used for the quantitative evaluation of LV systolic function from a mechanical view. The PSL is obtained by combining afterload and strain data, which overcomes the effect of afterload on strain and better reflects LV contraction. The PSL evaluation of global myocardial work includes

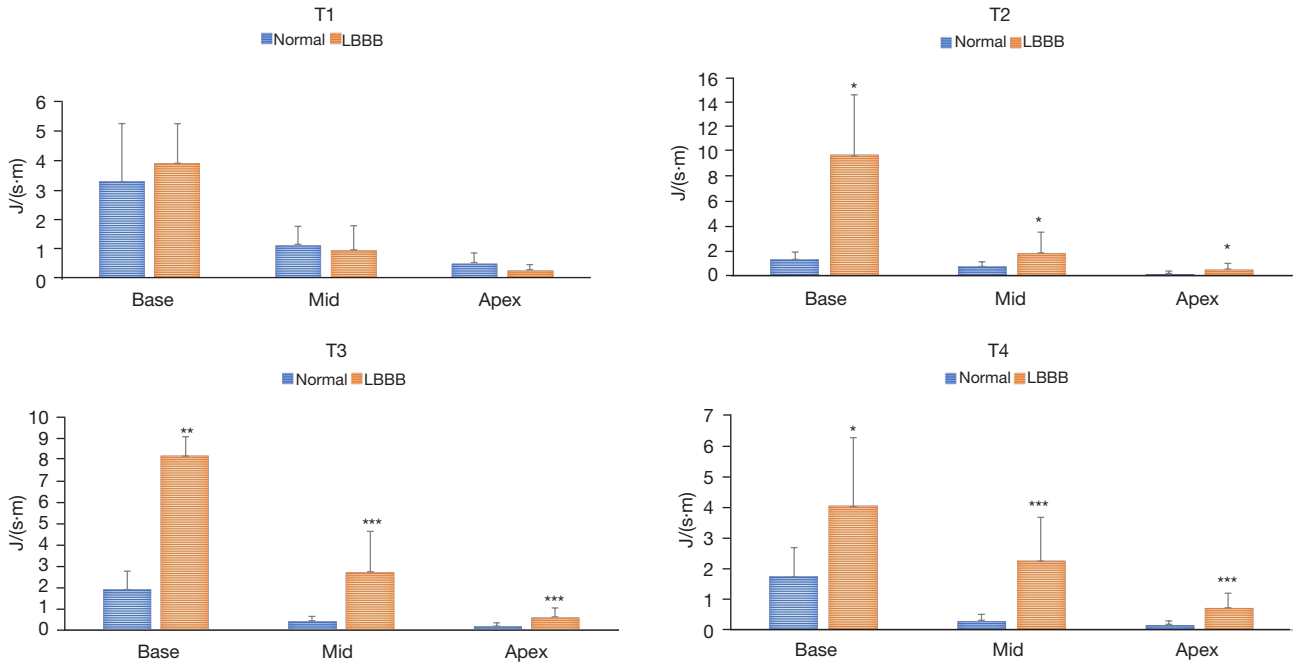

Figure 4 The EL-SUM in the basal (EL-base), mid (EL-mid), and apical (EL-apex) segments of the left ventricle in the normal group and the iLBBB group (J/(s·m)). *P<0.05; **P<0.01; ***P<0.001. T1, early diastole period; T2, late-diastole period; T3, isovolumic-systole period; T4, rapid-ejection period; LBBB, left bundle branch block; EL-SUM, summation of energy loss.

Table 6 Interobserver and intraobserver reproducibility of myocardial work and EL measurements

Variables	Interobserver			Intraobserver		
	ICC	95% CI	P	ICC	95% CI	P
GLS	0.875	0.578 to 0.968	<0.001*	0.851	0.512 to 0.961	<0.001*
GWI	0.901	0.672 to 0.976	<0.001*	0.981	0.927 to 0.995	<0.001*
GCW	0.986	0.946 to 0.997	<0.001*	0.997	0.911 to 0.994	<0.001*
GWW	0.999	0.997 to 1.000	<0.001*	0.999	0.991 to 0.999	<0.001*
GWE	0.960	0.847 to 0.990	<0.001*	0.964	0.864 to 0.991	<0.001*
EL-AVE T1	0.978	0.914 to 0.994	<0.001*	0.886	0.609 to 0.970	<0.001*
EL-AVE T2	0.998	0.990 to 0.999	<0.001*	0.995	0.979 to 0.999	<0.001*
EL-AVE T3	1.000	0.999 to 1.000	<0.001*	0.998	0.992 to 1.000	<0.001*
EL-AVE T4	0.999	0.996 to 1.000	<0.001*	0.999	0.998 to 1.000	<0.001*
EL-SUM T1	0.853	0.414 to 0.980	<0.001*	0.885	0.606 to 0.970	<0.001*
EL-SUM T2	0.998	0.991 to 0.999	<0.001*	0.963	0.859 to 0.991	<0.001*
EL-SUM T3	0.996	0.983 to 0.999	<0.001*	0.999	0.997 to 1.000	<0.001*
EL-SUM T4	0.866	0.482 to 0.968	0.006*	0.872	0.517 to 0.978	0.003*

*P<0.05. EL, energy loss; ICC, interclass correlation coefficient; CI, confidence interval; GLS, global longitudinal strain; GWI, global work index; GCW, global constructive work; GWW, global waste work; GWE, global work efficiency; EL-AVE, average energy loss; EL-SUM, summation of energy loss.

the following parameters: the GWI, GCW, GWW, and GWE. The GWI represents the total work in the PSL area formed by mitral valve closure to opening and is also known as the sum of the myocardial work. GCW represents the myocardial work done by the shortening of the myocardium in the systolic phase and the elongation of the myocardium in the isovolumic diastolic phase, which is also known as the assisting work of left ventricular ejection. GWW represents the myocardial work done by the elongation of the myocardium during the systolic phase and the shortening of the myocardium during the isovolumic diastolic phase, which is the adverse work of ventricular ejection. GWE is calculated using the following formula: GWE = GCW/(GCW + GW) × 100%. (19).

We found that the GLS, the GWI, and GWE were significantly lower in the iLBBB group than in the control group, while GWW was significantly higher. iLBBB induces dyssynchrony in the left ventricular free wall relative to the septum, which leads to a pathological lag in the electromechanical activity of the posterior or lateral walls of the LV, reducing the septal support for left ventricular contraction in turn. The paradoxical motion of the septum significantly affects cardiac electrophysiology, contractile function, and local myocardial perfusion, and reduces myocardial deformation capacity. Thus, the left ventricular myocardial work indices of GWI and GWE decrease. Dyssynchrony in the left ventricular free wall causes additional energy to be expended in ineffective ejection, increasing GWW and decreasing myocardial work efficiency.

Strain describes the deformation of the myocardium that occurs during the cardiac cycle in the longitudinal, circumferential, and radial planes. During systole, the LV undergoes longitudinal and circumferential shortening and radial thickening. GLS is a remarkably robust systolic function marker (21). In our study, we found that the LVEF was similar in the two groups, but the GLS in the iLBBB group was significantly reduced. This was consistent with the findings of Ashraf *et al.* (10), who examined 2,522 patients over a follow-up period of 8.4±3.2 years and found that the incidence rate of cardiomyopathy in patients with iLBBB over 1 year was 3.2% and that over 10 years was 9.1%; moreover, 7% of the patients developed heart failure in 1 year, and 18% of the patients developed heart failure over 10 years. This indicates that the cardiac function of most patients with iLBBB is normal in the early stage and develops slowly. Conversely, in our study, even when the LVEF of the two groups was similar (i.e., even when both were in the normal range), the GLS, GWI, GWW, and GWE differed significantly, which shows that these myocardial work parameters are more sensitive than is LVEF in the early stage of the disease.

We observed myocardial work indices in 17 segments of the LV in both groups and found that the MWI in the septum, basal inferior and mid-inferior segments, apical anterior segment, apical lateral segment, and apex were significantly decreased in the iLBBB group. A previous study (22) reported that the typical echocardiographic findings of patients with LBBB were septal flash and apical rocking. Septal flash (22) is a premature shortening of the septum during the T3 that affects myocardial contraction in this segment. Our study also found that the septal MWIs (of both the anterior and posterior septum) were decreased in patients with iLBBB. Apical rocking (23) is a back-and-forth motion of the LV apex related to the mutual stretching of the opposing walls. This back-and-forth motion affects the contraction of the apex.

In this study, we observed a significant decrease in the MWIs of the apical anterior, apical lateral, and apical septal segments, and the apex. The uncoordinated septal motion also affects the activity of its neighboring segments. In this study, a decrease in the MWIs was also observed in both the basal inferior and mid-inferior segments. It has also been noted in the literature that the typical longitudinal strain curve changes in the LBBB include (I) the early shortening of at least 1 basal or mid-ventricular segment in the septal wall and the early stretching of at least 1 basal or mid-ventricular segment in the lateral wall, (II) early septal peak shortening (within the first 70% of the ejection phase), and (III) lateral wall peak shortening after aortic valve closure (24). In the LBBB mode, the left ventricular lateral wall motion is also uncoordinated; however, in the patients with iLBBB enrolled in our study, the MWIs did not change significantly in the basal and mid-lateral segments, but the MWI of the apical lateral segment was significantly affected, which may be related to the longer electromechanical conduction delay in this segment.

In this study, the patients with iLBBB had increased EL-SUM and EL-AVE during the T2, T3, and T4 compared to the controls; meanwhile, energy consumption in all the segments was similarly higher in iLBBB than control in these 3 phases, most notably during the T3. The dyssynchrony of electrical activity in patients with iLBBB causes the premature contraction of the basal or intermediate segments of the septum and the stretching of the basal or intermediate segments of the lateral wall during T3 (23). This mechanical dyssynchrony inevitably leads to an elevated

LV EL. As previously reported (25), LBBB mainly leads to a prolongation of the T3 and a decrease in the peak rate of pressure rise (dP/dtmax). The EL is increased by sharp increases in velocity, which cause more turbulence during the T3. This was also observed in patients with uremic cardiomyopathy (26). Our study also found the EL-SUM and EL-AVE to be increased during the T3. During the T4, the patients with idiopathic LBBB showed significant apical rocking (23) in the LV, indicating mechanical dyssynchrony and more significant EL. We also discovered that the EL-SUM of the apex rose most during the T3 and T4, which corresponds to apical rocking during the systolic period.

Septal flash refers to an early septal thickening/thinning during the isovolumic contraction period due to the septal contraction against a reduced load in patients with iLBBB (22). Such brief motion fluctuations result in increased EL due to variations in blood flow shear during the systolic period, which explains the EL-SUM changes in the middle segment. Our study also found that mechanical dyssynchrony was not limited to the systolic period. The shortening of the lateral wall of the LV occurs after aortic valve closure (27), and the delayed excitation of the lateral wall in patients with iLBBB affects the mitral valve and the papillary muscle, causing mitral regurgitation and dragging on the mitral valve, which hinders the filling of the LV (28). During the isovolumic relaxation period, the aortic and mitral valves are still closed, there is little residual blood flow in the chambers, the blood flow changes slowly, and EL is at the lowest stage of the cardiac cycle. Due to LV compliance, LV EL is minimal in early diastole. However, the mechanical asynchrony of the LV lateral wall and its effect on the mitral valve causes a considerable increase in LV EL in mid-to-late diastole. When blood flows from the left atrium into the LV, high-speed blood flow diffuses from the basal to the intermediate and apical segments, causing shear friction with a larger shear angle at the base and a smaller shear angle at the intermediate and apical segments (29), which in turn results in an increase in EL in mid-to-late diastole, with the basal segment being much more pronounced than other segments. The phenomenon mentioned above was observed in this investigation, demonstrating impaired myocardial work and blood flow efficiency in patients with idiopathic LBBB.

Study limitations

This research was a pilot study with a limited number of participants. In the future, studies with larger cohorts need to be conducted to verify the myocardial work changes and EL changes in patients with iLBBB.

Conclusions

Patients with idiopathic LBBB have increased GWW, decreased GLS, a decreased GWI, and decreased GWE, but have normal LVEF. The MWI dropped markedly in the septum and the apex. To further understand the decline of its work efficiency, we used VFM and found that EL mainly occurs during the T2, T3, and T4, especially during T3because of mechanical dyssynchrony. Thus, EL and PSL can be used to evaluate diastolic and systolic hemodynamic functioning in individuals with iLBBB.

Acknowledgments

Funding: The present study was supported by the National Natural Science Foundation of China (No. 81871359) and by the Natural Science Foundation of Jiangsu Province (No. BK20191496).

Footnote

Conflicts of Interest: All authors have completed the ICMJE uniform disclosure form (available at https://qims.amegroups.com/article/view/10.21037/qims-22-284/coif). The authors have no conflict of interest to declare.

Ethical Statement: The authors are accountable for all aspects of the work in ensuring that questions related to the accuracy or integrity of any part of the work are appropriately investigated and resolved. The study was conducted in accordance with the Declaration of Helsinki (as revised in 2013). The study was approved by the Institutional Review Board of The First Affiliated Hospital of Nanjing Medical University, and informed consent was provided by all individual participants.

References

1. Akhtari S, Chuang ML, Salton CJ, Berg S, Kissinger KV, Goddu B, O'Donnell CJ, Manning WJ. Effect of isolated left bundle-branch block on biventricular volumes and ejection fraction: a cardiovascular magnetic resonance assessment. J Cardiovasc Magn Reson 2018;20:66.
2. Vernooy K, Verbeek XA, Peschar M, Crijns HJ, Arts T, Cornelussen RN, Prinzen FW. Left bundle branch block induces ventricular remodelling and functional septal hypoperfusion. Eur Heart J 2005;26:91-8.
3. Cvijic M, Duchenne J, Ünlü S, Michalski B, Aarones M, Winter S, Aakhus S, Fehske W, Stankovic I, Voigt JU. Timing of myocardial shortening determines left ventricular regional myocardial work and regional remodelling in hearts with conduction delays. Eur Heart J Cardiovasc Imaging 2018;19:941-9.
4. Francia P, Balla C, Paneni F, Volpe M. Left bundle-branch block--pathophysiology, prognosis, and clinical management. Clin Cardiol 2007;30:110-5.
5. Eriksson P, Hansson PO, Eriksson H, Dellborg M. Bundle-branch block in a general male population: the study of men born 1913. Circulation 1998;98:2494-500.
6. Fahy GJ, Pinski SL, Miller DP, McCabe N, Pye C, Walsh MJ, Robinson K. Natural history of isolated bundle branch block. Am J Cardiol 1996;77:1185-90.
7. Auffret V, Martins RP, Daubert C, Leclercq C, Le Breton H, Mabo P, Donal E. Idiopathic/Iatrogenic Left Bundle Branch Block-Induced Reversible Left Ventricle Dysfunction: JACC State-of-the-Art Review. J Am Coll Cardiol 2018;72:3177-88.
8. Smiseth OA, Aalen JM. Mechanism of harm from left bundle branch block. Trends Cardiovasc Med 2019;29:335-42.
9. Sze E, Dunning A, Loring Z, Atwater BD, Chiswell K, Daubert JP, Kisslo JA, Mark DB, Velazquez EJ, Samad Z. Comparison of Incidence of Left Ventricular Systolic Dysfunction Among Patients With Left Bundle Branch Block Versus Those With Normal QRS Duration. Am J Cardiol 2017;120:1990-7.
10. Ashraf H, Agasthi P, Siegel RJ, Pujari SH, Allam M, Shen WK, Srivathsan K, Sorajja D, Masry HE, Freeman WK, Mookadam F, Mulpuru S, Arsanjani R. Natural history and clinical significance of isolated complete left bundle branch block without associated structural heart disease. Anatol J Cardiol 2021;25:170-6.
11. Delise P, Rivetti L, Poletti G, Centa M, Allocca G, Sitta N, Cati A, Turiano G, Lanari E, Zeppilli P, Sciarra L. Clinical and Prognostic Significance of Idiopathic Left Bundle-Branch Block in Young Adults. Cardiol Res Pract 2021;2021:6677806.
12. Wong KK, Tu J, Kelso RM, Worthley SG, Sanders P, Mazumdar J, Abbott D. Cardiac flow component analysis. Med Eng Phys 2010;32:174-88.
13. Hong GR, Pedrizzetti G, Tonti G, Li P, Wei Z, Kim JK, Baweja A, Liu S, Chung N, Houle H, Narula J, Vannan MA. Characterization and quantification of vortex flow in the human left ventricle by contrast echocardiography using vector particle image velocimetry. JACC Cardiovasc Imaging 2008;1:705-17.
14. Itatani K, Okada T, Uejima T, Tanaka T, Ono M, Miyaji K, Takenaka K. Intraventricular flow velocity vector visualization based on the continuity equation and measurements of vorticity and wall shear stress. Japanese Journal of Applied Physics 2013;52:07HF16.
15. Stugaard M, Koriyama H, Katsuki K, Masuda K, Asanuma T, Takeda Y, Sakata Y, Itatani K, Nakatani S. Energy loss in the left ventricle obtained by vector flow mapping as a new quantitative measure of severity of aortic regurgitation: a combined experimental and clinical study. Eur Heart J Cardiovasc Imaging 2015;16:723-30.
16. Brignole M, Auricchio A, Baron-Esquivias G, Bordachar P, Boriani G, Breithardt OA, Cleland J, Deharo JC, Delgado V, Elliott PM, Gorenek B, Israel CW, Leclercq C, Linde C, Mont L, Padeletti L, Sutton R, Vardas PE, Guidelines ESCCfP, Zamorano JL, Achenbach S, Baumgartner H, Bax JJ, Bueno H, Dean V, Deaton C, Erol C, Fagard R, Ferrari R, Hasdai D, Hoes AW, Kirchhof P, Knuuti J, Kolh P, Lancellotti P, Linhart A, Nihoyannopoulos P, Piepoli MF, Ponikowski P, Sirnes PA, Tamargo JL, Tendera M, Torbicki A, Wijns W, Windecker S, Document R, Kirchhof P, Blomstrom-Lundqvist C, Badano LP, Aliyev F, Bansch D, Baumgartner H, Bsata W, Buser P, Charron P, Daubert JC, Dobreanu D, Faerestrand S, Hasdai D, Hoes AW, Le Heuzey JY, Mavrakis H, McDonagh T, Merino JL, Nawar MM, Nielsen JC, Pieske B, Poposka L, Ruschitzka F, Tendera M, Van Gelder IC, Wilson CM. 2013 ESC Guidelines on cardiac pacing and cardiac resynchronization therapy: the Task Force on cardiac pacing and resynchronization therapy of the European Society of Cardiology (ESC). Developed in collaboration with the European Heart Rhythm Association (EHRA). Eur Heart J 2013;34:2281-329.
17. Lang RM, Badano LP, Mor-Avi V, Afilalo J, Armstrong A, Ernande L, Flachskampf FA, Foster E, Goldstein SA, Kuznetsova T, Lancellotti P, Muraru D, Picard MH,

Rietzschel ER, Rudski L, Spencer KT, Tsang W, Voigt JU. Recommendations for cardiac chamber quantification by echocardiography in adults: an update from the American Society of Echocardiography and the European Association of Cardiovascular Imaging. Eur Heart J Cardiovasc Imaging 2015;16:233-70.
18. Aalen J, Storsten P, Remme EW, Sirnes PA, Gjesdal O, Larsen CK, Kongsgaard E, Boe E, Skulstad H, Hisdal J, Smiseth OA. Afterload Hypersensitivity in Patients With Left Bundle Branch Block. JACC Cardiovasc Imaging 2019;12:967-77.
19. El Mahdiui M, van der Bijl P, Abou R, Ajmone Marsan N, Delgado V, Bax JJ. Global Left Ventricular Myocardial Work Efficiency in Healthy Individuals and Patients with Cardiovascular Disease. J Am Soc Echocardiogr 2019;32:1120-7.
20. Wang X, Hong J, Zhang T, Xu D. Changes in left ventricular and atrial mechanics and function after dialysis in patients with end-stage renal disease. Quant Imaging Med Surg 2021;11:1899-908.
21. Potter E, Marwick TH. Assessment of Left Ventricular Function by Echocardiography: The Case for Routinely Adding Global Longitudinal Strain to Ejection Fraction. JACC Cardiovasc Imaging 2018;11:260-74.
22. Parsai C, Bijnens B, Sutherland GR, Baltabaeva A, Claus P, Marciniak M, Paul V, Scheffer M, Donal E, Derumeaux G, Anderson L. Toward understanding response to cardiac resynchronization therapy: left ventricular dyssynchrony is only one of multiple mechanisms. Eur Heart J 2009;30:940-9.
23. Voigt JU, Schneider TM, Korder S, Szulik M, Gürel E, Daniel WG, Rademakers F, Flachskampf FA. Apical transverse motion as surrogate parameter to determine regional left ventricular function inhomogeneities: a new, integrative approach to left ventricular asynchrony assessment. Eur Heart J 2009;30:959-68.
24. Risum N, Jons C, Olsen NT, Fritz-Hansen T, Bruun NE, Hojgaard MV, Valeur N, Kronborg MB, Kisslo J, Sogaard P. Simple regional strain pattern analysis to predict response to cardiac resynchronization therapy: rationale, initial results, and advantages. Am Heart J 2012;163:697-704.
25. Hultgren HN, Craige E, Fujii J, Nakamura T, Bilisoly J. Left bundle branch block and mechanical events of the cardiac cycle. Am J Cardiol 1983;52:755-62.
26. Hong J, Zhang Y, Wang Y, Zhang T, Wang X, Xu D. Influence of a single hemodialysis on left ventricular energy loss and wall shear stress in patients with uremic cardiomyopathy assessed with vector flow mapping. Quant Imaging Med Surg 2022;12:4059-68.
27. Risum N, Tayal B, Hansen TF, Bruun NE, Jensen MT, Lauridsen TK, Saba S, Kisslo J, Gorcsan J 3rd, Sogaard P. Identification of Typical Left Bundle Branch Block Contraction by Strain Echocardiography Is Additive to Electrocardiography in Prediction of Long-Term Outcome After Cardiac Resynchronization Therapy. J Am Coll Cardiol 2015;66:631-41.
28. Grines CL, Bashore TM, Boudoulas H, Olson S, Shafer P, Wooley CF. Functional abnormalities in isolated left bundle branch block. The effect of interventricular asynchrony. Circulation 1989;79:845-53.
29. Elbaz MS, van der Geest RJ, Calkoen EE, de Roos A, Lelieveldt BP, Roest AA, Westenberg JJ. Assessment of viscous energy loss and the association with three-dimensional vortex ring formation in left ventricular inflow: In vivo evaluation using four-dimensional flow MRI. Magn Reson Med 2017;77:794-805.

Cite this article as: Gao Y, Zhang Y, Tang Y, Wu H, Xu F, Hong J, Xu D. Myocardial work and energy loss of left ventricle obtained by pressure-strain loop and vector flow mapping: a new perspective on idiopathic left bundle branch block. Quant Imaging Med Surg 2023;13(1):210-223. doi: 10.21037/qims-22-284

